Scientific paper

The Enhancement of H_2O_2/UV AOPs for the Removal of Selected Organic Pollutants from Drinking Water with Hydrodynamic Cavitation

Matej Čehovin,[1,2,*] Alojz Medic,[2] Boris Kompare[1,†] and Andreja Žgajnar Gotvajn[3]

[1] *Faculty of Civil and Geodetic Engineering, University of Ljubljana, Hajdrihova 28, 1000 Ljubljana, Slovenia*

[2] *MAK CMC Water Technology Ltd., Tbilisijska ulica 81, 1000 Ljubljana, Slovenia*

[3] *Faculty of Chemistry and Chemical Technology, University of Ljubljana, Večna pot 113, 1000 Ljubljana, Slovenia*

** Corresponding author: E-mail: Matej.Cehovin@mak-cmc.si; phone: +386-(0)41-676-020*

Received: 21-07-2016

Abstract

Drinking water contains organic matter that occasionally needs to be treated to assure its sufficient quality and safety for the consumers. H_2O_2 and UV advanced oxidation processes (H_2O_2/UV AOPs) were combined with hydrodynamic cavitation (HC) to assess the effects on the removal of selected organic pollutants. Water samples containing humic acid, methylene blue dye and micropollutants (metaldehyde, diatrizoic acid, iohexol) were treated first by H_2O_2 (dosages from 1 to 12 mg L^{-1}) and UV (dosages from 300 to 2800 mJ cm^{-2}) AOPs alone and later in combination with HC, generated by nozzles and orifice plates (4, 8, 18 orifices). Using HC, the removal of humic acid was enhanced by 5–15%, methylene blue by 5–20% and metaldehyde by approx. 10%. Under favouring conditions, i.e. high UV absorbance of the matrix (more than 0.050 cm^{-1} at a wavelength of 254 nm) and a high pollutant to oxidants ratio, HC was found to improve the hydrodynamic conditions in the photolytic reactor, to improve the subjection of the H_2O_2 to the UV fluence rate distribution and to enhance the removal of the tested organic pollutants, thus showing promising potential of further research in this field.

Keywords: Advanced oxidation, Dissolved Organic Carbon, Hydrogen peroxide, Hydrodynamic cavitation, Methylene Blue, Ultraviolet

1. Introduction

Organic matter is omnipresent within the sources of drinking water originating from natural processes. Studies are showing that concentrations of total and dissolved organic carbon (TOC and DOC, respectively) in the sources of drinking water have been actually increasing during the last few decades.[1] Although water treatment processes are being researched and developed constantly, natural organic matter (NOM) still presents a challenge due to its effects on water during its collection, treatment and distribution: (i) colourisation, smell and "earthy" taste of the water;[1] (ii) increased demand of chemicals used in water treatment to achieve the treatment goal, since NOM react with the aforementioned chemicals;[1,2] (iii) formation of complexes with (heavy) metals and organic micropollutants that are more difficult to remove;[1,3] (iv) formation of oxidation and disinfection by-products (DBPs) – especially with chlorine – which are proven to have harmful (carcinogenic, reproductive etc.) effects on the consumers and are contributing to the formation of biodegradable organic compounds that can result in microbiological growth in the distribution system, potentially decreasing the water quality even below allowed standards.[1,2,4] The quest of sufficient NOM treatment is therefore almost always present, especially when untreated water contains more than 2 mg L^{-1} of TOC.[2,4,5]

† Prof. Dr. Boris Kompare, Professor of Environmental Engineering; deceased 23 October 2014

Synthetic organic compounds (SOCs) originating from various anthropogenic activities induce reactions in the organisms for which no adequate biological response is available seeing that their presence in the environment is relatively new and no mechanism could be developed to adapt to them so quickly.[6–8] These chemicals show mostly long-term detrimental effects (carcinogenicity, mutagenicity, genotoxicity, disruption of endocrine system etc.), with already very low concentrations in the range of μg L^{-1} to trigger them; therefore they are called micropollutants.[8,6,7] Due to the presence of numerous species, their harmful effects are multiplied by the so-called "cocktail effect".[9] Their persistency in the environment and the bioaccumulation are of further concern, as well as the challenges of drinking and waste water treatment, since they are poorly responsive to the removal by traditional technologies (e.g. coagulation, flocculation, oxidation, filtration, biological treatment etc.).[8,6,9]

Advanced oxidation processes (AOPs) have already been well-researched and practically applied for the treatment of recalcitrant natural and synthetic organic pollutants in drinking water.[1,2,4,10] Characteristically, they take place by oxidizing chemical species in water matrix with the highly reactive and non-selective hydroxyl radicals (HO•) which are considered to be the strongest technically applicable oxidants in water treatment with the oxidation potential of 2.81 V.[10] For drinking water treatment, HO• are commonly generated by the combination of strong oxidants, such as ozone (O_3, 2.07 V) and hydrogen peroxide (H_2O_2, 1.78 V) or combination of the latter with the UV irradiation, although with much higher UV dosages than used for disinfection (40 mJ cm^{-2}).[10,11] With the advances in the efficiency of the equipment used, H_2O_2/UV AOPs are nowadays considered both technically and economically attractive for full-scale applications worldwide.[1,2,4,6,10] Nevertheless, to enhance the treatment efficiency and to reduce material and energy inputs (reduced costs per unit of treated volume) extensive research is dedicated to finding synergistic effects of combined treatment processes or to optimising and intensifying the performance of already established technologies.

Hydrodynamic cavitation (HC) has been intensively researched during the past two to three decades as a potential AOP, as it induces effects typical of very low frequency ultrasound applications (range of 10–20 kHz) already investigated in details.[12,13] Cavitation in general represents the formation, growth, cyclic compression and the rarefaction with the terminal implosive collapse of water vapour bubbles inside otherwise homogenous media, due to the decrease of static pressure below vapour pressure caused by changes in flow geometry (hydrodynamic cavitation), ultrasound, boiling, fast moving objects or particles (ship propellers, pumps), laser and similar.[14,15] When cavitation bubbles collapse, extreme temperatures (up to 5000 °C inside cavitation bubble) and pressures (approx. 500–1000 bar) can exist locally for micro- to milliseconds.[15,16] Under these conditions the following reactions can proceed, with the thermal dissociation of water vapour inside cavitation bubble representing the first step (chemical Equation /1/):[15]

$$H_2O \rightarrow H\bullet + HO\bullet \quad (1)$$
$$O_2 \rightarrow 2\ O\bullet \quad (2)$$
$$H\bullet + H_2O \rightarrow HO\bullet + H_2 \quad (3)$$
$$O\bullet + H_2O \rightarrow 2\ HO\bullet \quad (4)$$
$$H\bullet + O_2 \rightarrow HOO\bullet \quad (5)$$
$$2\ HO\bullet \rightarrow H_2O_2 \quad (6)$$
$$2\ HOO\bullet \rightarrow H_2O_2 + O_2 \quad (7)$$

In the presence of cavitation H_2O_2 can dissociate to form HO• radicals, however it can also produce less oxidative species in parallel:[17]

$$H_2O_2 \rightarrow HO\bullet + HO\bullet \quad (8)$$
$$HO\bullet + HO\bullet \rightarrow H_2O_2 \quad (9)$$
$$H_2O_2 + HO\bullet \rightarrow HO_2\bullet + H_2O \quad (10)$$
$$HO_2\bullet + HO_2\bullet \rightarrow H_2O_2 + O_2 \quad (11)$$
$$HO\bullet + O_2 \rightarrow HO_2\bullet + O\bullet \quad (12)$$

Apart from the chemical effects, e.g. the formation of hydroxyl (HO•) and peroxyl (HOO•) radicals as well as hydrogen peroxide duo to the homolytic cleavage of water molecules, HC induces mechanical effects on bulk liquid in the form of severe turbulence, shear stresses, velocity and pressure pulsations, shock waves, evaporation and the condensation of the solution constituents etc.[12,15] HC can therefore be applied also to improve the mass transfer of the applied oxidants or as a hybrid (complementary) process, including disinfection.[12,18–20]

In this study, the effects of HC on H_2O_2/UV AOPs were investigated. HC was generated at the entry point to photolytic plug-flow reactor and the treatment performance was studied on the samples containing methylene blue (MB) dye (an industrial dye, but with a typical reactivity to HO• and therefore highly suitable to assess and compare AOPs), humic acid (HA) as a source of DOC (representing NOM), and selected micropollutants: metaldehyde (common and widespread pesticide), diatrizoic acid and iohexol (X-ray contrast agents used in medical applications).[1,21–24]

2. Experimental

2. 1. Set-up

The system is represented in Figure 1. Sample water from the tank was drawn via a frequency-controlled circulation pump with 0.75 kW installed power. System was equipped with power consumption meters that enabled the calculation of electrical energy per order of the pollutant removal (E_{EO}). Water flow, temperature and pressures (at the entry and the exit of UV reactor) were continuously

measured with precise electronic instruments. The acquired data were stored in the computer for analyses. H_2O_2 (30% w/w, Ph. Eur., USP by AppliChem, Darmstadt, Germany) was dosed into the system via a precise metering pump prior to the photolytic UV reactor, from where the water was returned to the tank. Water flow was maintained in the range of 0.20–0.25 L s^{-1}, depending on the applied treatment configuration.

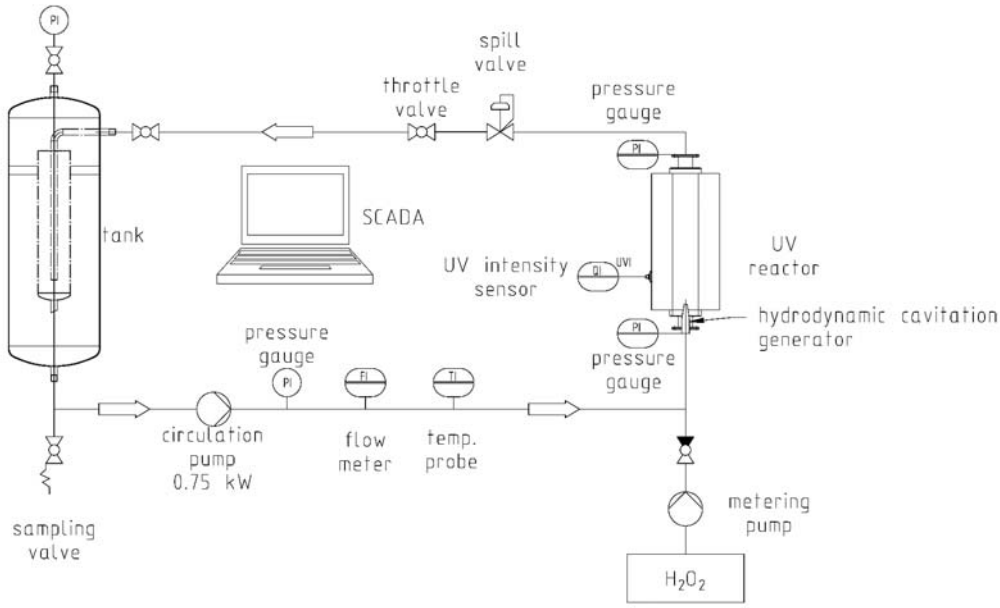

Figure 1. Design of the experimental set-up.

UV reactor (type E10-PH by Wedeco, Germany) consisted of an annular vertical quartz glass pipe (diameter = 61 mm, length = 970 mm), serving as a plug flow

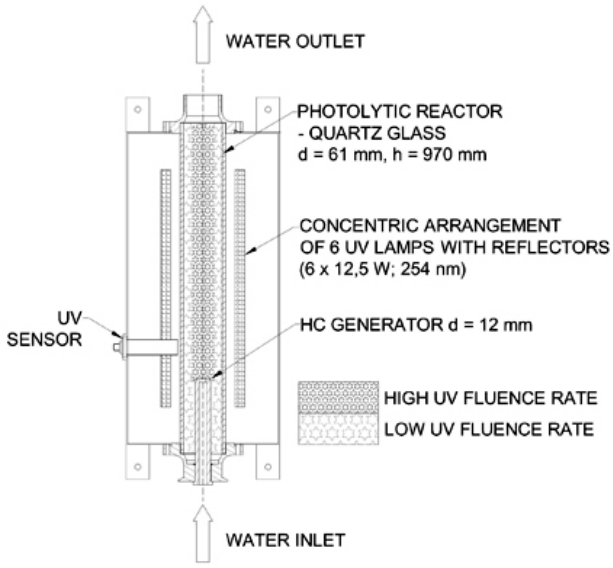

Figure 2. Photolytic UV reactor cross-section with HC generator (illustration).

photolytic reactor (as shown in Figure 2), with the arrangement of 6 concentric monochromatic UV lamps, each with power of 12.5 W at a wavelength of 254 nm. The UV lamps were placed outside the quartz glass pipe with reflectors directing the photons towards the centre of the pipe and thus concentrating the UV irradiance in the zone with the highest axial velocity and distributing the UV fluence rate across the cross-section following turbulent hydrodynamic flow pattern (as illustrated in Figure 2). The system was equipped with an UV irradiance sensor (type SO13599 by Wedeco, Germany; Resolution 0.1 W m^{-2}; Accuracy ± 3%), with 160° opening angle. UV reactor enabled installation of HC generation elements at the entry to the reactor (Figure 1). All the experimental configurations, presented in Table 1, were used as H_2O_2/UV AOPs alone and with the application of HC.

2. 2. Calibration of Dose-performance of the UV System

Methylene blue water solutions are relatively poorly decolorized by the UV light itself, but are very reactive with HO• generated by, for example, H_2O_2/UV AOPs.[23] Therefore, MB can be used as a benchmark test for H_2O_2/UV AOPs.[23,25] In parallel, experiments were run in the H_2O_2/UV experimental set-up and on UV-collimated beam device (CBD, type 11–1 by Wedeco, Germany) in petri dishes, where accurate applied UV dosages can be established based on the exposure time of the sample and the known geometry of the petri dish and the UV fluence rate distribution.[23] For a known UV dosage from CBD tests, MB degradation can be determined using the UV-VIS spectroscopy by the reduction of light absorbance (at a wavelength of 610 nm in this research). Results of the CBD tests were compared to the absorbance reduction ob-

tained in the experimental H_2O_2/UV set-up, thus enabling its dose-performance calibration.

2. 3. Hydrodynamic Cavitation

One of the benefits of HC application is its scale-up possibility.[12,13,15] Therefore, this potential was utilized and the experiments were performed using 83 L of the total volume for humic acid and micropollutant removal as well as 50 L for methylene blue removal. The intensity of cavitation phenomena is described by dimensionless cavitation number (C_v):

$$C_v = (P_2 - P_v)/(1/2 \cdot \rho \cdot v^2) \quad (13)$$

where P_2 is absolute downstream pressure (backpressure) [Pa], P_v is vapour pressure at a given temperature [Pa], ρ is water density at a given temperature [kg m^{-3}] and v is flow velocity [m s^{-1}] at the throat of the constriction. Another important parameter is the number of passes (*NOP*) through the HC generator.[26] Relatively low *NOP* was used in this research, namely up to 9 for humic acid and micropollutants removal and between 9 and 12 for methylene blue removal. From the previous research reported in the literature,[15,26,27] several dozen to several hundreds of even thousands of passes are required to generate chemical effects that result in detectable amount of radical species to assure chemical oxidation by HC. For *NOP* in the range up to several dozen mechanical effects of HC would prevail and this has been the case in the present research. Simultaneously, *NOP* is also a characteristic of H_2O_2/UV AOPs without HC, the figure representing the number of passes through the UV reactor (Table 1). Characteristically, experiments using HC involve external temperature management of the system (e.g. heat exchangers etc.).[16,26,28] However, due to the relatively large bulk of the sample volumes (50–83 L), low *NOP* and short experiment duration, the system was not additionally cooled-down and the temperatures were kept in the range of 23–27 °C for all of the applied configurations.

Various geometry of HC generators was also tested (nozzle with single opening and orifice plates with 4, 8 and 18 openings, Figure 3 and Table 2) in relation to the treatment performance of methylene blue decolourization. For the experiments with humic acid and micropollutants only an orifice plate with 8 openings (n = 8) was used for H_2O_2/UV AOPs coupled with HC.

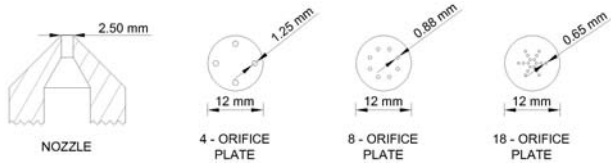

Figure 3: Geometry of the applied HC generators.

2. 4. Sample Preparation

Experiments were performed using samples of tap water to which prepared solutions of selected pollutants were added. Tap water was supplied from deep wells with practically no turbidity (< 0.06 NTU), no iron and manganese (both < 0.01 mg L^{-1}), practically no colour (< 0.001 cm^{-1}) and low DOC (< 1.0 mg L^{-1}); however with relatively high concentration of carbonate species (total hardness = 3.0–3.3 mmol L^{-1} as $CaCO_3$) as the potential HO• scavengers (analyses from tap water supplier Stadtwerke Herford GmbH, Herford, Germany; obtained

Table 1. Characteristics of the experimental conditions.

Pollutant	Parameter for evaluation of removal efficiency	Parameter value at thestart of the experiment	Applied H_2O_2 dosage [mg L^{-1}]	Applied UV dosage [mJ cm^{-2}]	*NOP* [/]
Methylene blue	Absorbance at λ = 610 nm [cm^{-1}]	0.358–0.375	5.0	500–2800	12
			10.0	500–1900	9
Humic acid	DOC [mg L^{-1}]	1.1–3.4	4.0–12.0	300–1800	9
Micropollutants (metaldehyde, diatrizoic acid, iohexol)	Concentration [μg L^{-1}]	8.2–11.0	10.0	450–2700	9

Table 2. Features of the applied HC generators.

HC generator type	Number of openings n [/]	Opening diameter [mm]	Total cross-section [mm^2]	Average calculated water velocity at constriction [m/s]	C_v [/]	Power consumption of the circulation pump [kW]
Nozzle	1	2.50	4.9	40.7	0.17–0.23	0.75
Orifice plate	4	1.25	4.9	40.7	0.16–0.20	0.73
Orifice plate	8	0.90	4.9	41.1	0.14–0.18	0.68
Orifice plate	18	0.65	6.0	41.5	0.12–0.22	0.55

23.11.2013). pH of the solutions was not modified throughout the experiments and was ranging from 7.7 to 7.8.

MB solution for each experiment was prepared by dissolving 0.200–0.210 g of MB hydrate as provided (by Sigma-Aldrich) in 500 mL of demineralized water and added to 50 L of the sample. This resulted in the initial light absorbance of the sample ranging between 0.358–0.375 cm^{-1} at λ = 610 nm. UVA_{254} was in the range 0.168 ± 0.015 cm^{-1} (the UV light transmission at λ = 254 m of approx. 68% per 1 cm) at the beginning of the experiments.

The solution of humic acid (HA, technical grade, Sigma-Aldrich, CAS: 1415-93-6) was prepared by dissolving HA in demineralized water in volumetric flasks. Mixture was kept in the dark at 20 ± 1 °C for 48 h and mixed completely every 12 h prior to the filtration on laboratory filters (Whatman Ashless Grade 589/3, pore size 2 μm) to remove suspended particles. HA solution was then added to the water sample used in the experimental set-up with 83 L of total volume and DOC concentrations ranging from 1 to 3 mg L^{-1}. UVA_{254} was 0.067 ± 0.02 cm^{-1} (the UV light transmission at λ = 254 m of approx. 86% per 1 cm) at the beginning of the experiments.

The stock solution of the micropollutants was prepared from the reagents as provided, all analytical standard grade: (i) Metaldehyde (by Fluka – Sigma-Aldrich, CAS: 9002-91-9); (ii) Diatrizoic acid (by Sigma-Aldrich, CAS: 117-96-4); (iii) Iohexol (by Sigma-Aldrich, CAS: 66108-95-0). After the preparation, the stock solution was kept in the dark at 4 ± 1 °C. 90 mL of the stock solution was added to each of the investigated samples in the experiments using 83 L of tap water, resulting in starting concentrations of the respective micropollutants between 8.2 and 11.0 μg L^{-1}. UVA_{254} was, compared to MB and HA experiments, relatively very low in the range of 0.017 ± 0.02 cm^{-1}.

2. 5. Analytical Methods

UV-VIS spectrometry was performed on a laboratory spectrophotometer (type HACH DR5000, Germany) in 10 mm quartz cuvette with the calibration performed using deionised water (Water for chromatography, LC-MS Grade, LiChrosolv by Merck Millipore). For MB experiments and to detect the colour removal, an absorbance wavelength of λ = 610 nm (A_{610}) was used. For all the experiments the UV absorbance was measured at a wavelength of λ = 254 nm (UVA_{254}). Hydrogen peroxide was determined using a titanium (IV) oxysulfate spectrophotometric method at a wavelength λ = 400 nm. DOC concentrations [mg L^{-1}] were determined according to DIN EN 1484 standard, using Shimadzu TOC 5050 analyser.

Analyses of metaldehyde were performed on GC-MS after pre-concentration by solid-phase extraction. GC-MS system consisted of a gas chromatograph 6890 and a mass selective detector MSD 5973, both from Agilent Technologies (Waldbronn, Germany). Chromatographic separation was done on the Rxi-5ms column (by Restek GmbH, Bad Homburg, Germany). 500 mL of water sample were pre-concentrated on 100 mg of a polymeric material (Strata X, Phenomenex). Elution was done with 4 mL of dichloromethane which was then evaporated in a gentle stream of nitrogen to a final volume of 500 μL, and then an aliquot of 10 μL was injected into a GC-MS system. Chromatographic separation was done on Restek Rxi-5 MS column (30 m × 0.25 mm × 0.25 μm). Oven temperature started at 45 °C which was held for 2 minutes and then raised to 160 °C at a rate of 10 °C min^{-1}. After 3 min at 160 °C, the temperature was raised to 280 °C at a rate of 20 °C min^{-1} and again held for 5 minutes. The quantification was done against the calibration in MilliQ water. Due to the relatively high concentrations used for the experiments, samples were diluted 1:10 prior to the extraction and thus the levels of quantification (LOQ) for metaldehyde were 0.5 μg L^{-1}.

The analyses of diatrizoic acid and iohexol were performed on HPLC-MS-MS after the pre-concentration by the solid-phase extraction. HPLC-MS-MS system which consisted of a liquid chromatograph 1290 Infinity from Agilent Technologies (Waldbronn, Germany) coupled via an electrospray interface to an API 5500 tandem mass spectrometer (AB Sciex, Langen, Germany). The chromatographic separation was done on a Thermo Fisher Hypersil Gold column (100 mm × 2.1 mm, 3 μm particle size). 200 mL of water sample were adjusted to a pH of 3 and pre-concentrated on 200 mg of a styrene-divinylbenzene copolymer (SDB1, Fisher Scientific). Elution was done with 5 mL of methanol and subsequently with 5 mL of acetonitrile. The elution solvents were evaporated to dryness and the dry residue reconstituted with 500 μL of HPLC grade water. Then an aliquot of 100 μL was injected into a HPLC-MS-MS system. Chromatographic separation was performed by using an aqueous solution of 5 mM ammonium formate and 0.1% formic acid (eluent A), and a solution of 5 mM ammonium formate and 0.1% formic acid in methanol (eluent B) as the elution solvents. The elution gradient started at 95% of eluent A, gradually changed to 15% of eluent B in first 7 minutes, and to 100% of eluent B up to 13 min, then stayed constant for 6 min, and finally adjusted back to 95% of eluent A between min 19 and min 20. Flow rate of the eluent was 0.25 mL min^{-1} and the temperature of the column oven was set to 40 °C. The detection of both target compounds was done in positive mode applying an ionisation voltage of 5.5 kV. Before and after each series of samples, a control sample and a blank sample were run. Quantification was done against the calibration in MilliQ water. Due to the relatively high concentrations used for the experiments, samples were diluted 1:10 prior to the extraction and thus LOQ were 0.1 μg L^{-1} for each of the X-ray contrast agents.

2. 6. Removal of the Selected Organic Pollutants

A decrease in the concentrations of the organic pollutants used herein was described through pseudo-first order kinetic equation:

$$\ln([x_t]/[x_0]) = -k \cdot t \qquad (14)$$

where x_0 is the initial value of the evaluated parameter (A_{610} [cm^{-1}], DOC [mg L^{-1}], micropollutants concentration [μg L^{-1}]; Table 1), x_t the value of the same evaluated parameter at experiment time t [min] and k [min^{-1}] the pseudo-first order rate constant. To express the degree of correlation between the removal rate and the applied UV dosages and due to the fact that linear regression could be applied (in logarithmic scale), determination coefficients (R^2) were calculated for each individual pollutant.

3. Results and Discussion

3. 1. Decolourization of Methylene Blue Solution

As presented in Table 3 and Figures 4–5, the applied H_2O_2/UV AOPs resulted in 40% discoloration of the MB solution at a wavelength of λ = 610 nm at H_2O_2 dosage of 5 mg L^{-1} and the UV dosage of 2800 mJ cm^{-2} and 60% discoloration of the MB solution at a wavelength of λ = 610 nm at H_2O_2 dosage of 10 mg L^{-1} and the UV dosage of 1900 mJ cm^{-2}. In both cases, the overall decolourization of MB was enhanced by the application of HC by up to approx. 15% under the conditions described herein. The results of HC coupled with AOPs are expressed as an average of all the applied HC experiment configurations (Table 2). From the results obtained, the application of HC obviously improved mass transfer of H_2O_2 and its exposure to UV irradiation, based on changes in hydrodynamic characteristic in the UV reactor and due to the mechanisms induced by the HC which consequently yielded more HO and hence improved MB decolourization.

UVA_{254} remained unchanged (0.168 ± 0.015 cm^{-1}) throughout the treatment with 5 mg L^{-1} of H_2O_2, independent of UV dosage. On the contrary, UVA_{254} was reduced by 20–24% throughout the treatment with 10 mg L^{-1} of H_2O_2 and UV dosage of 1900 mJ cm^{-2}. This reduction was

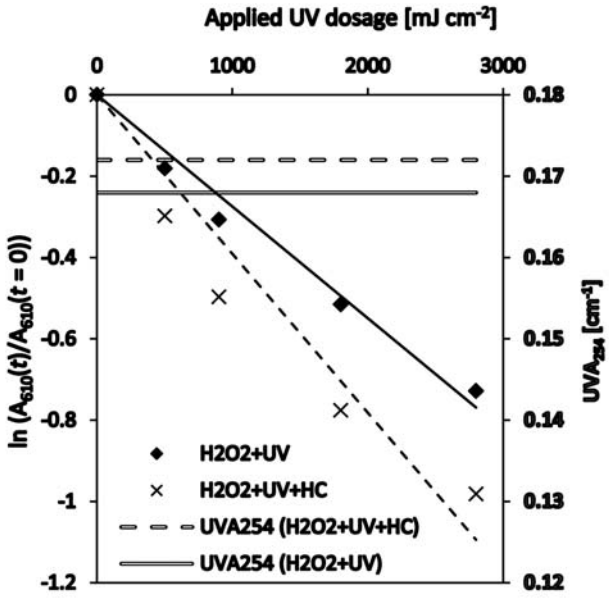

Figure 4. Decolourization of the MB solution as a function of applied UV dosage; H_2O_2 dosage 5 mg L^{-1}.

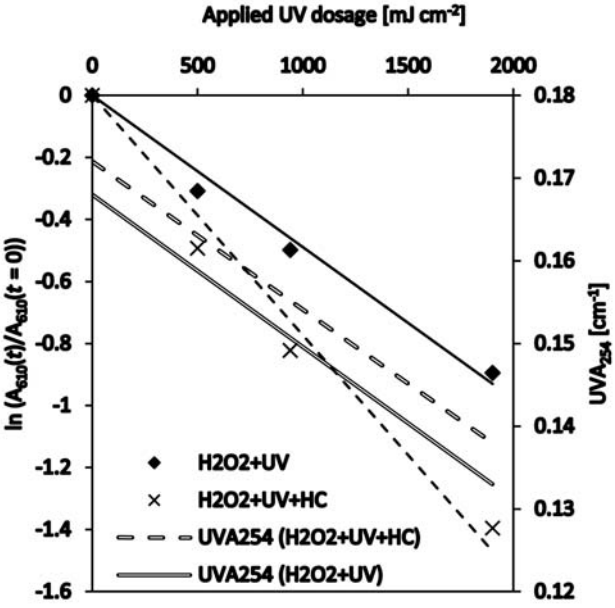

Figure 5. Decolourization of the MB solution as a function of applied UV dosage; H_2O_2 dosage 10 mg L^{-1}.

Table 3. Kinetic parameters and efficiency of MB solution decolourization.

Experimental configuration	Applied H_2O_2 dosage [mg L^{-1}]	Applied UV dosage [mJ cm^{-2}]	k [10^{-4}, min^{-1}]	R^2 [/]	Average A_{610} decolourization efficiency [%]	UVA_{254} [cm^{-1}] before the treatment	UVA_{254} [cm^{-1}] after the treatment
H_2O_2 + UV	5	2800	2.75	0.98	40.3	0.168 ± 0.015	0.168 ± 0.015
H_2O_2 + UV + HC	5	2800	3.91	0.92	53.4	0.172 ± 0.015	0.172 ± 0.015
H_2O_2 + UV	10	1900	4.89	0.98	59.1	0.168 ± 0.015	0.133 ± 0.013
H_2O_2 + UV + HC	10	1900	7.74	0.97	74.8	0.172 ± 0.015	0.138 ± 0.010

evident in the same range for H_2O_2/UV AOPs alone or coupled with HC. Therefore, the treatment predominately resulted in decolourization at λ = 610 nm, i.e. the decomposition of MB molecules, however, the oxidation products have obviously remained as chromophores (aromatic or molecules with multiple chemical bond) that absorb UV light.[1] To increase UVA_{254} reduction, higher dosages of H_2O_2 should be applied.

3. 2. Influence of HC Generator Geometry on MB Solution Decolourization Efficiency

According to the results of already conducted research on HC, geometry of the generator or constriction (e.g. orifice plates, Venturi, rotation blades etc.) can significantly change the performance of the treatment.[13,26,29] Predictions or model forecasts and evaluations on the subject are for now virtually impossible due to numerous influencing parameters and their variations that still have not been researched to the extent allowing for generalisation.[27,30] Besides the geometry of the HC generators (e.g. hydraulic radii, the number and the distribution of openings of the orifice plates, converging and diverging angles of Venturi injectors etc.), the influence of the inlet and recovered pressures of HC, presence and concentrations of dissolved gasses and process intensifying chemical agents etc., are among the variables that affect the process.[26]

The kinetics of MB discolouration using different HC generators are presented in Figures 6 and 7. The differences in the MB decolourization were not found to be significant (± 5–10% between different applied HC generator geometries), however, the power consumption of the circulation pump to produce C_v in the same range could differ by as much as 40% between them (Table 2), with the 18-opening orifice plate (n = 18) consuming the least and the nozzle (n = 1) the most energy. Of the HC generators tested, the nozzle also resulted in lower MB decolourization than the other geometries (Figures 6 and 7), especially at H_2O_2 dosage of 10 mg L^{-1}, while orifice plates with n = 4 and 8 were performing better (both in the same order of magnitude) and the orifice plate with n = 18 in the range between the other types. Depending on the observations made, the results of other research[13,26] can be supported and we could not generally and conclusively declare the best performing HC generator geometry, although from the MB decolourization results and electrical energy consumption, orifice plate with 8 openings was found to be optimum following the conditions of the experiment. Derived for the results obtained herein, the evaluations of the most optimal HC generator type and the geometry intended for a hybrid AOP are suggested for each experimental set-up configuration, type and concentration of the pollutants, characteristics of the water matrix and the dosages of the simultaneously applied oxidants (e.g. H_2O_2, UV, O_3 etc.).

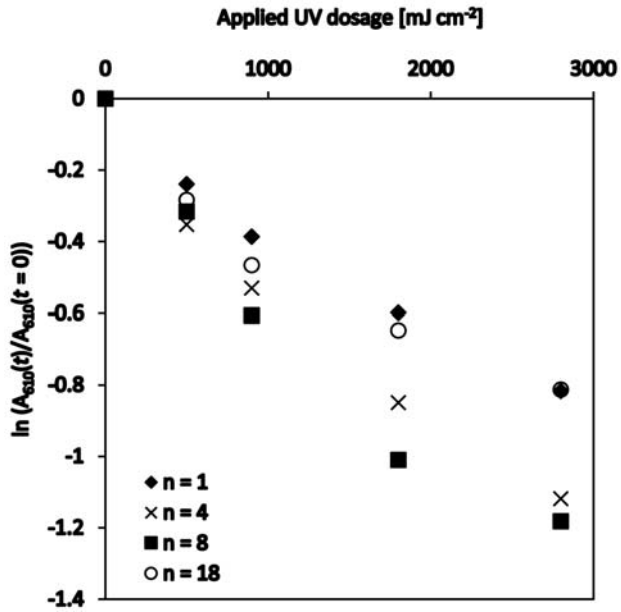

Figure 6. MB decolourization using different HC generator geometry (*n* represents the number of openings of the HC generator, as described in Figure 3 and Table 2); H_2O_2 dosage 5 mg L^{-1}.

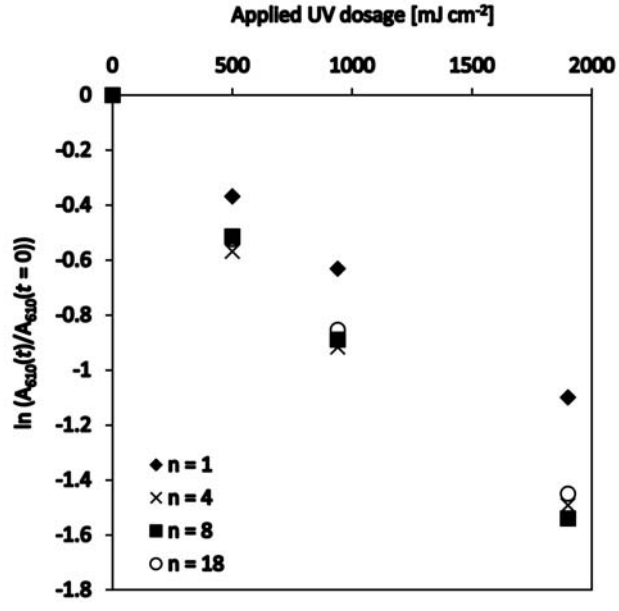

Figure 7. MB decolourization using different HC generator geometry (*n* represents the number of openings of the HC generator, as described in Figure 3 and Table 2); H_2O_2 dosage 10 mg L^{-1}.

3. 3. DOC Removal from Humic Acid Solution

As presented in Figure 8, DOC oxidation in this experiment was apparently a two-stage reaction – initially, at relatively low UV and H_2O_2 dosages up to 300 mJ cm^{-2} and 4 mg L^{-1}, respectively, the removal rate was

significantly higher than at the increased dosages of the applied oxidants. The first stage represents conditions of the relatively high DOC concentrations and the relatively high UVA_{254} values at the start of the experiments (Table 4). The second stage represents the conditions of the relatively lower DOC concentrations and lower UVA_{254}. H_2O_2/UV AOPs alone were able to reduce approx. 15–23% of DOC under herein described conditions, whereas coupling the processes with HC resulted in approx. 30–50% better DOC reduction, comparatively (Table 4). Apparently, the application of HC resulted in improved DOC removal, especially in the first stage, which again leads to the understanding of advantages of such hybrid H_2O_2/UV AOPs. Moreover, due to relatively high UVA_{254} in the first stage, the benefits of HC application are emphasized in less favourable conditions for UV photolysis. Related to UVA_{254}, both experiment configurations gave a comparable range of reduction, eventually approx. 45% at the highest dosages of the applied oxidants (Table 4).

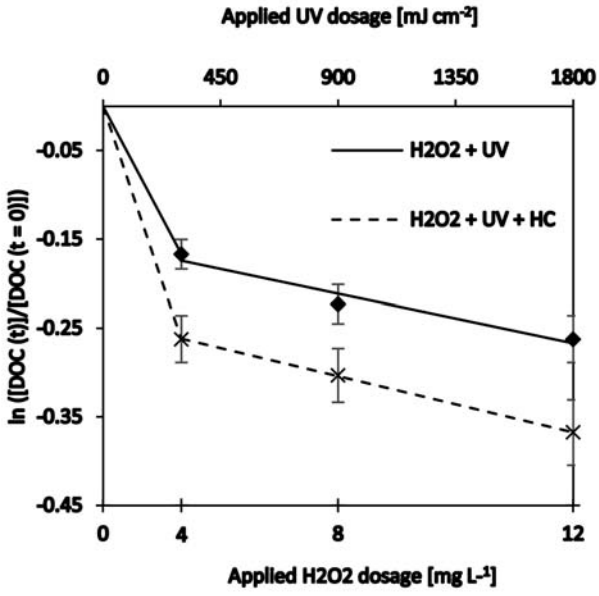

Figure 5. Decolourization of the MB solution as a function of applied UV dosage; H_2O_2 dosage 10 mg L^{-1}.

3. 4. Removal of Micropollutants

These sets of experiments were performed by the application of 10 mg L^{-1} of H_2O_2 and only UV dosages were varied between 450 and 2700 mJ cm^{-2}. Contrary to the experiments with MB and HA, water matrix used herein (described in Section 2.4), had only a very low UVA_{254}, namely 0.017 ± 0.02 cm^{-1}. Diatrizoic acid and iohexol (referred to as contrast agents) are both relatively highly susceptible to treatment by the UV irradiation and H_2O_2/UV AOPs.[23] The required UV dosages for achieving the same degree of removal in the performed experiments were approx. 4–4.5 fold lower than the ones for the treatment of metaldehyde, which is much more recalcitrant, as presented in Figure 9. Moreover, the investigated contrast agents show roughly the same removal rates during the herein described conditions, therefore the representation in Figure 9 relates to both. Since the LOQs possible by the analytical methods used (0.5 μg L^{-1} for metaldehyde and 0.1 μg L^{-1} for the contrast agents) were reached by applying the relatively low UV dosages in the case of the contrast agents, their removal was only observed in the range up to 450 mJ cm^{-2}, where already 90–95% removal had been reached. The removal of metaldehyde of the same order of magnitude was only reached applying the UV dosages in the range of 2000–2700 mJ cm^{-2}.

The application of HC was not found to improve the removal of the contrast agents under the conditions described herein or was even lowering the removal rate by approx. 5%. In the case of metaldehyde that is much more persistent, HC was able to improve the removal rate by approx. 10% at the UV dosages above 1350 mJ cm^{-2}. Nevertheless, taking into account the uncertainties related to the methods applied, distinct benefits of HC applications were not as obvious as in the case of MB or HA removal (Sections 3.1.1 and 3.1.3). Here the pollutants' concentrations were higher by about 3 orders of magnitude and the UVA_{254} was comparatively much higher, with the latter representing much less favourable conditions for photolysis based H_2O_2/UV AOPs. In the case of the micropollutants removal, water matrix was of much lesser UVA_{254}, and the ratios of the dosages of applied oxidants over the quantity of the pollutants were approx. 3 orders of magnitude higher than in the case of MB and HA experiments. Altogether, these conditions did not emphasize the potential be-

Table 4. Efficiency of DOC removal and UVA_{254} reduction.

Experimental configuration	Applied H_2O_2 dosage [mg L^{-1}]	Applied UV dosage [mJ cm^{-2}]	Average DOC removal efficiency [%]	UVA_{254} before the treatment [cm^{-1}]	UVA_{254} after the treatment [cm^{-1}]	Average UVA_{254} reduction [%] configuration
H_2O_2 + UV	4	300	15.4	0.066 ± 0.003	0.062 ± 0.002	5.4
H_2O_2 + UV + HC	4	300	23.1	0.068 ± 0.003	0.063 ± 0.002	7.4
H_2O_2 + UV	8	900	20.0	0.062 ± 0.002	0.050 ± 0.002	24.3
H_2O_2 + UV + HC	8	900	26.2	0.063 ± 0.002	0.051 ± 0.002	24.3
H_2O_2 + UV	12	1800	23.1	0.050 ± 0.002	0.036 ± 0.002	44.9
H_2O_2 + UV + HC	12	1800	30.8	0.051 ± 0.002	0.037 ± 0.002	45.3

nefits of HC effects that were much more obvious for the other experiments described herein.

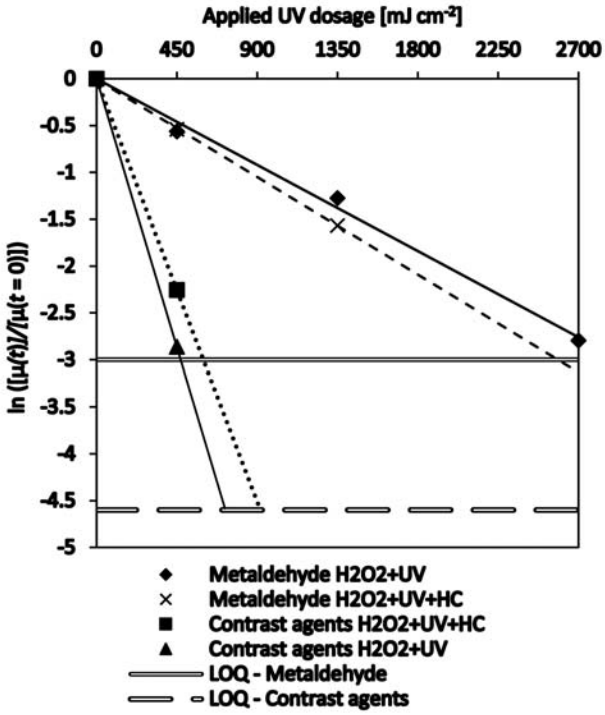

Figure 9. Micropollutants removal as a function of applied UV dosage; H_2O_2 dosage 10 mg L^{-1}; [μ] represents concentration of respective micropollutant.

3. 5. Influence of HC on Hydrodynamic and Photolytic Conditions Inside the UV Reactor

Much effort is put into the design of the efficient fluence rate distribution in the photolytic UV reactors, where the optimal distribution of UV lamps and flow pattern play a major role.[31] The latter issue is commonly addressed applying various flow diverters, baffle plates or similar flow conditions optimizers. Potentially, the application of HC can be considered among the measures of addressing these challenges, as shown herein.

When operated without the HC, the flow pattern through the UV photolytic reactor used herein was subjected to typical plug-flow conditions and turbulent velocity profile, as presented in Figure 10 a.). Reynolds number was calculated using the term:

$$Re = v \cdot d/\nu \qquad (15)$$

where v [m s^{-1}] is the mean flow velocity in the cross-section of the pipe with the diameter d [m] and in which case ν [m^2 s^{-1}] is the kinematic viscosity of the water (approx. 10^{-6} m^2 s^{-1} at 20 °C).[32] The mean velocity of the water flow was quasi-constant in the range of 0.68–0.72 m s^{-1} and Re in the range of 4200–5200. Based on the theoretical grounds, the mean flow velocity in the cross-section ranges between 0.80–0.87 of the maximum flow velocity in the centre of the pipe, which causes turbulent eddies near the pipe walls.[32] These eddies are dissipated in the flow as it passes along the axis of the reactor and result only in relatively low radial and counter-current turbulence. Therefore, in the Sections 1, 2 and 3 of the UV reactor (Figure 10 a.), along its longitudinal axis, the flow conditions can be considered equal.

HC severely changed the hydrodynamic conditions inside the chamber where it took place. It has to be noted that the hydrodynamic phenomena caused by HC are modelled by the complex hydraulic models and is the subject of numerous past and current research.[33–35] The description herein is provided solely for the readers to conceive the matter in an easier way. At the throat of the constriction the calculated v was approx. 40 m s^{-1} (Table 2) and Re was approx. $1.02 \cdot 10^5$, representing very intensive turbulence. As the flow cross-section increased to the one of the photolytic reactor (Figure 10 b., cavitation zone between Sections 2 and 3), the turbulent effect diminished along the longitudinal axis and returned to plug-flow conditions (Figure 10 b., Section 3), which is typical of the flow without the application of HC. If the Borda-Carnot model was assumed and generalized to this case, the length of the dissipation of the turbulence after the HC generators was approx. 8–10 fold of the difference between downstream and upstream pipe diameter (HC generator in this case), before the expansion.[32]

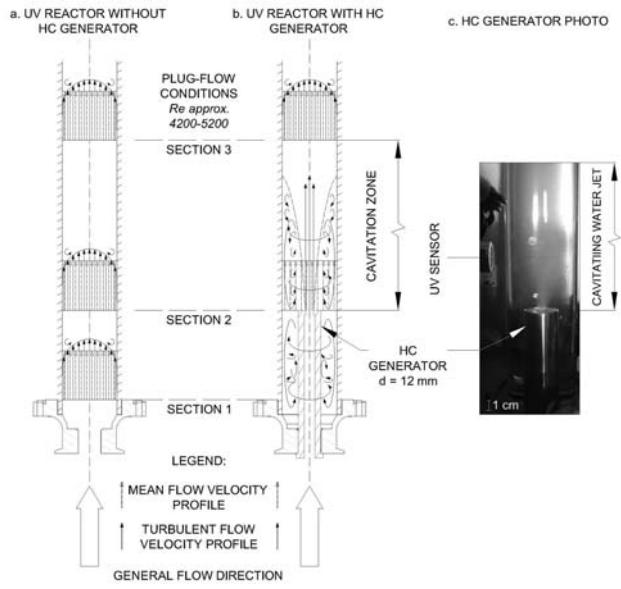

Figure 10. Illustration of flow pattern conditions inside UV photolytic reactor: a. Plug flow conditions throughout the longitudinal axis of the UV reactor (Sections 1–3) without the application of HC; b. Severe radial and counter-current turbulence in Sections 1 and 2 when HC was applied; c. Photo of the photolytic reactor with the UV lamps removed and a visible HC generator with the cavitating water jet.

Between Sections 1 and 2 and especially between Sections 2 and 3 in Figure 10 b.), the influence of HC was expressed in intensive radial and counter-current turbulence. Nevertheless, the mean velocity across the UV reactor in Sections 2 and 3 is maintained the same (mass conservation). The behaviour of such a water flow pattern was obviously improving the mass transfer of H_2O_2 related to the reactions in the unevenly distributed UV fluence rate as illustrated in Figure 2. From the results presented in Section 3.1, H_2O_2 mass transfer could be improved thereby, especially in the conditions of the relatively high UVA_{254} and pollutants concentrations (MB and HA).

Related to the influence of HC on photolytic reactions, Figure 11 displays the UV light fluence rates E_o [W m–2] at λ = 254 nm during the MB treatment by H_2O_2/UV AOPs alone and coupled with HC, measured by the UV sensor in the cavitation zone (Figure 10). Based on the theoretical aspects described by Bolton[31], for the same (relatively high) range of UVA_{254} of the matrix (0.168 ± 0.015 cm^{-1}), lower values of the senor readings in HC-coupled configurations represent the conditions, in which more UV photons were consumed by the water matrix. This implies more reactions of UV with H_2O_2 to yield HO• or the direct photolysis of the pollutants (the other way around, less UV photons reached the UV sensor), which correlates with the higher removal rates of the MB when HC was applied. Although the differences in the UV sensor readings between H_2O_2/UV AOPs and these coupled with HC are only in the range of 5–10% (Figure 11), this value was sufficient enough to increase the MB decolourization by approx. 15%.

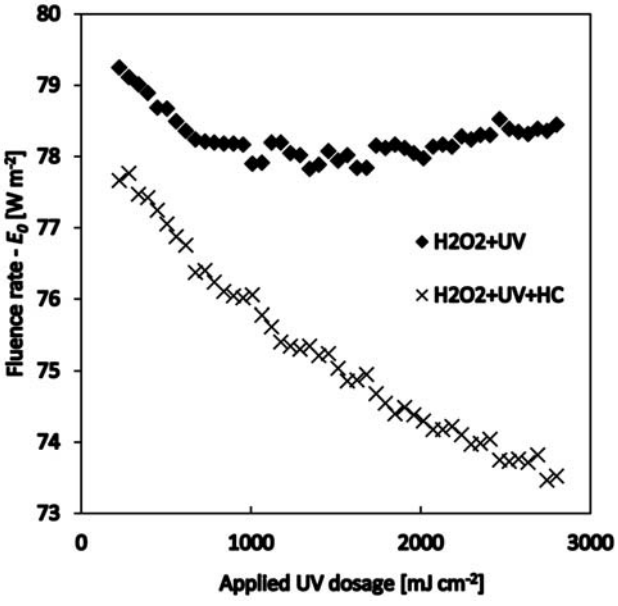

Figure 11. Comparison of the fluence rate readings of the UV sensor for MB decolourization experiments; H_2O_2 dosage = 5 mg L^{-1}, UVA_{254} = 0.168 ± 0.015 cm^{-1}.

On the opposite side, micropollutants experiments were performed using water matrix with a very low UVA_{254}, i.e. 0.017 ± 0.02 cm^{-1}. Much higher absolute fluence rate values for these sets of experiments compared to MB decolourization, in the range of approx. 184–196 W m^{-2} and 73–79 W m^{-2}, respectively, are a consequence of low UVA_{254} (much less UV photons are absorbed by the matrix). As shown in Figure 12, the sensor readings were practically the same for H_2O_2/UV AOPs alone or these coupled with HC, or the latter were higher. On the grounds explained above, these observations can be correlated to the results of the micropollutants removal, where the application of HC did not contribute significantly to the overall removal rates.

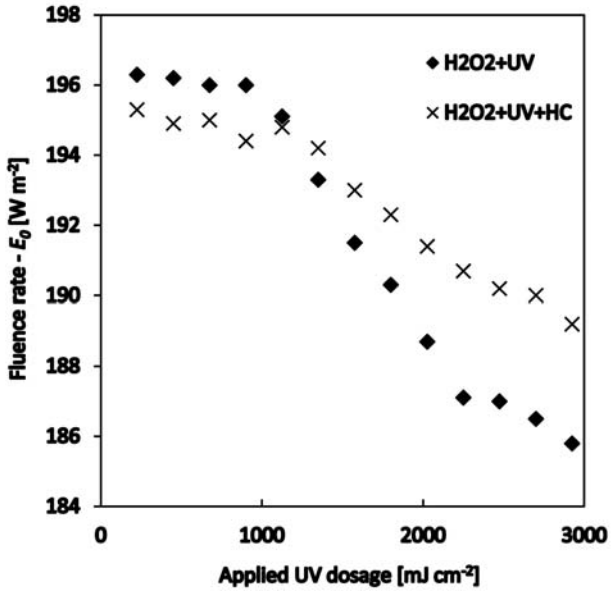

Figure 12. Comparison of the fluence rate readings of the UV sensor for micropollutants removal experiments; H_2O_2 dosage = 10 mg L^{-1}, UVA_{254} = 0.017 ± 0.02 cm^{-1}.

3. 6. Energy Efficiency of the Treatment

To assess the energy efficiency, electric energy per order (or 90%) of removal E_{EO} [kWh m^{-3} $order^{-1}$] of the selected evaluated parameter was calculated using the term:

$$E_{EO} = P \cdot t / (V \cdot \log ([x_0]/[x_t])) \quad (16)$$

where P [kW] is the electrical power consumption of the experimental setup, measured using the power meters installed on the experimental set-up, x_0 is the initial value of the evaluated parameter (A_{610} [cm^{-1}], DOC [mg L^{-1}], micropollutants concentration [μg L^{-1}]; Table 1) and x_t the

value of the same evaluated parameter at experiment time t [h]. The P for the experiments without the application of HC was 0.73 kW, whereas the P for the HC-coupled experiments was 0.98 kW, including the power consumption of the UV photolytic reactor.

The application of HC requires additional driving force to reach its adequate conditions compared to H_2O_2/UV AOPs alone. For comparability, all results of HC treatment are expressed using an orifice plate with 8 openings (n = 8). UV/H_2O_2 AOPs alone could be operated under 1 bar of pressure in the photolytic reactor, whereas the application of HC to reach C_v conditions described in Table 2, required pressures of 6–8 bar at the inlet of HC generators, thus increasing the energy consumption by approx. 25% to increase the pressure from the circulation pump. Nevertheless, as provided in Table 6, in the case of the MB decolourization and the DOC removal, H_2O_2/UV configuration applying HC as a hybrid process was as energy efficient as the H_2O_2/UV AOPs alone. In these two cases the overall removal efficiencies were also increased by the application of HC, justifying the additional energy input. On the other hand, micropollutants in general, and especially the contrast agents, were more efficiently removed without the application of HC. Regarding metaldehyde, further research would be required using different geometries of the HC generators to establish the optimum configuration and possibly reach the same or lower E_{EO} than for the H_2O_2/UV AOPs alone.

Table 6. Electric energy per order of removal of the selected evaluated parameter.

Experimental configuration	E_{EO} [kWh m^{-3} order^{-1}]			
	MB decolourization (λ = 610 nm)	Humic acid removal (as DOC)	Metaldehyde removal	Contrast agents removal
H_2O_2 + UV	46.2	80.1	11.0	2.4
H_2O_2 + UV + HC	46.6	76.7	12.0	4.0

4. Conclusions

The effects of the treatment by H_2O_2/UV AOPs alone and those coupled with hydrodynamic cavitation on the decolourization of methylene blue solution, removal of dissolved organic carbon from the samples containing humic acid and the removal of metaldehyde, diatrizoic acid and iohexol as micropollutants were investigated. From the conducted research and under herein described conditions, the application of HC resulted in:

- Increased turbulence throughout much of the plug-flow UV reactor (cavitation zone), with much higher dispersion and diffusion in the form of increased radial and counter-current turbulent eddies, thus improving the exposure of the sample to the uneven UV fluence rate distribution at a given cross-section of the reactor in the cavitation zone;
- Improved H_2O_2 mass transfer and a higher yield of radical species (HO• and HOO•) that was expressed in the increased removal rate of the investigated organic pollutants.

The potential benefits of the HC application as a hybrid process to H_2O_2/UV AOPs were emphasized in the conditions of relatively:

- High UV absorbance (at λ = 254 nm) and colourization of the matrix, i.e. unfavourable conditions for the efficient fluence rate distribution in the photolytic reactor;
- High pollutant concentrations;
- Low dosages of H_2O_2 and UV;
- Low ratio of (photo-) oxidants dosages to pollutant concentration.

Due to the fact that HC enables scale-up from laboratory- and pilot-size to full-scale applications, further research and development of the HC generators geometry and the layout of the installations (optimized hydrodynamic conditions) is possible, yielding potentially more effective hybrid H_2O_2/UV AOPs for the removal of recalcitrant organic pollutants, especially in the conditions where the UV fluence rate distribution is less favourable. From the challenges awaited along this path, the issues of material wear and durability of the HC generators as well as the fact that exposure to adequate HC conditions requires additional energy input and conditions, limited by hydrodynamic parameters that potentially increase the treatment time to induce sufficient number of passes through the system, are among the ones that need to be addressed to increase the efficiency and practicability of this technology in the future. As shown by this study, coupling HC with H_2O_2/UV AOPs can be of interest for further research and development and could be transferred to practical or industrial applications.

5. Acknowledgements

Operation part financed by the European Union, European Social Fund (Young Researchers from the Economy program by SPIRIT Slovenia – Public Agency for Entrepreneurship, Internationalization, Foreign Investments and Technology of the Republic of Slovenia, Grant P-MR-10/30).

The authors would like to express gratitude to Xylem Services GmbH – Wedeco, Herford, Germany, for providing research facilities and especially to the Wedeco R&D laboratory team, Mr. Jens Scheideler, Ms. Carolin Meyer, Dr. Jörg Mielcke, Dr. Achim Ried, Mr. Harald Stapel, Mr. Sebastian Besser and others for their valuable contributions.

6. References

1. A. Matilainen, M. Sillanpää, *Chemosphere* **2010**, *80*, 351–365. http://dx.doi.org/10.1016/j.chemosphere.2010.04.067
2. A. D. Dotson, V. S. Keen, D. Metz, K. G. Linden, *Water Res.* **2010**, *44*, 3703–3713. http://dx.doi.org/10.1016/j.watres.2010.04.006
3. M. Bekbolet, C. S. Uyguner, H. Selcuk, L. Rizzo, A. D. Nikolaou, S. Meriç, V. Belgiorno, *Desalination* **2005**, *176*, 155–166. http://dx.doi.org/10.1016/j.desal.2004.11.011
4. S. Sarathy, M. Mohseni, *Water Res.* **2010**, *44*, 4087–4096. http://dx.doi.org/10.1016/j.watres.2010.05.025
5. USEPA, *Stage 2 Disinfectants and Disinfection Byproducts Rule*, Federal register, vol. 71, Number 18, United States Environmental Protection Agency, **2006**.
6. K. Ikehata, M. Gamal El-Din, S. A. Snyder, *Ozone Sci. Eng.* **2008**, *30*, 21–26. http://dx.doi.org/10.1080/01919510701728970
7. S. Singh, R. Seth, S. Tabe, P. Yang, *Ozone Sci. Eng.* **2015**, *37*, 323–329. http://dx.doi.org/10.1080/01919512.2014.998755
8. J. Derco, M. Valičková, K. Šilhárová, J. Dudáš, A. Luptáková, *Chem. Pap.* **2013**, *67*, 1585–1593. http://dx.doi.org/10.2478/s11696-013-0324-x
9. M. I. Vasquez, A. Lambrianides, M. Schneider, K. Kuemmerer, D. Fatta-Kassinos, *J. Hazard. Mater.* **2014**, *279*, 169–189. http://dx.doi.org/10.1016/j.jhazmat.2014.06.069
10. J. C. Crittenden, R. R. Trussell, D. W. Hand, K. J. Howe, G. Tchobanoglous (Ed.): *MWH's water treatment: principles and design*; John Wiley & Sons, Hoboken, USA, **2012**, pp. 507–643
11. S. Arrojo, Y. Benito, *Ultrason. Sonochem.* **2008**, *15*, 203–211. http://dx.doi.org/10.1016/j.ultsonch.2007.03.007
12. E. F. Karamah, S. Bismo, W. W. Purwanto, *Ozone Sci. Eng.* **2013**, *35*, 482–488. http://dx.doi.org/10.1080/01919512.2013.820640
13. S. Arrojo, Y. Benito, *Ultrason. Sonochem.* **2008**, *15*, 203–211. http://dx.doi.org/10.1016/j.ultsonch.2007.03.007
14. S. Parsons (Ed.): *Advanced Oxidation Processes for Water and Wastewater Treatment*; IWA Publishing, London, **2004**.
15. P. Braeutigam, Z.-L. Wu, A. Stark, B. Ondruschka, *Chem. Eng. Technol.* **2009**, *32*, 745–753. http://dx.doi.org/10.1002/ceat.200800626
16 Z.-L. Wu, B. Ondruschka, P. Bräutigam, *Chem. Eng. Technol.* **2007**, *30*, 642–648. http://dx.doi.org/10.1002/ceat.200600288
17. S. Raut-Jadhav, V.K. Saharan, D. Pinjari, S. Sonawane, D. Saini, A. Pandit, *J. Hazard. Mater.* **2013**, *261*, 139–147. http://dx.doi.org/10.1016/j.jhazmat.2013.07.012
18. K. K. Jyoti, A. B. Pandit, *Ultrason. Sonochem.* **2003**, *10*, 255–264. http://dx.doi.org/10.1016/S1369-703X(03)00116-5
19. D. Maslak, D. Weuster-Botz, *Eng. Life Sci.* **2011**, *11*, 350–358. http://dx.doi.org/10.1002/elsc.201000103
20. K. K Jyoti, A. B. Pandit, *Water Res.* **2004**, *38*, 2249–2258. http://dx.doi.org/10.1016/j.watres.2004.02.012
21. S. Semitsoglou-Tsiapou, M. R. Templeton, N. J. D. Graham, L. Hernández Leal, B. J. Martijn, A. Royce, J. C. Kruithof, *Water Res.* **2016**, *91*, 285–294. http://dx.doi.org/10.1016/j.watres.2016.01.017
22. K. Ikehata, N. Jodeiri Naghashkar, M. Gamal El-Din, *Ozone Sci. Eng.* **2006**, *28*, 353–414. http://dx.doi.org/10.1080/01919510600985937
23. H.-W. Yu, T. Anumol, M. Park, I. Pepper, J. Scheideler, S. A. Snyder, *Water Res.* **2015**, *81*, 250–260. http://dx.doi.org/10.1016/j.watres.2015.05.064
24. S.-L. Lee, S.-W. Liew, S.-T. Ong, *Acta Chim. Slov.* **2016**, *63*, 144–153. http://dx.doi.org/10.17344/acsi.2015.2068
25. E. J. Rosenfeldt, K. G. Linden, *Environ. Sci. Technol.* **2007**, *41*, 2548–2553. http://dx.doi.org/10.1021/es062353p
26. P. Braeutigam, M. Franke, Z.-L. Wu, B. Ondruschka, *Chem. Eng. Technol.* **2010**, 6, 932–940. http://dx.doi.org/10.1002/ceat.201000021
27. S. Arrojo, C. Nerín, Y. Benito, *Ultrason. Sonochem.* **2007**, *14*, 343–349. http://dx.doi.org/10.1016/j.ultsonch.2006.06.007
28. M. Franke, P. Braeutigam, Z.-L. Wu, Y. Ren, B. Ondruschka, *Ultrason. Sonochem.* **2011**, *18*, 888–894. http://dx.doi.org/10.1016/j.ultsonch.2010.11.011
29. M. Zupanc, T. Kosjek, M. Petkovšek, M. Dular, B. Kompare, B. Širok, M. Stražar, E. Heath, *Ultrason. Sonochem.* **2014**, *21*, 1213–1221. http://dx.doi.org/10.1016/j.ultsonch.2013.10.025
30. P. Braeutigam, Z.-L. Wu, A. Stark, B. Ondruschka, *Chem. Eng. Technol.* **2010**, *33*, 341–346. http://dx.doi.org/10.1002/ceat.200900434
31. J. R. Bolton, *Wat. Res.* **2000**, *34*, 3315–3324. http://dx.doi.org/10.1016/S0043-1354(00)00087-7
32. G. Bollrich (Ed): Technische Hydromechanik Band 1, Huss-Medien, Berlin, Germany, **2007**, pp. 88–241.
33. J. S. Krishnan, P. Dwivedi, V. S. Moholkar, *Ind. Eng. Chem. Res.* **2006**, *45*, 1493–1504. http://dx.doi.org/10.1021/ie050839t
34. K. Sampath Kumar, V. S. Moholkar, *Chem. Eng. Sci.* **2007**, *62*, 2698–2711. http://dx.doi.org/10.1016/j.ces.2007.02.010
35. V. S. Moholkar, A. B. Pandit, *Chem. Eng. Sci.* **2001**, *56*, 6295–6302. http://dx.doi.org/10.1016/S0009-2509(01)00253-6

Povzetek

Pitna voda vsebuje organske snovi, zaradi katerih je potrebno le-to v nekaterih primerih dodatno pripraviti, da vzdržujemo njeno ustrezno kakovost in varnost za uporabnike. Pri odstranjevanju modelnih organskih onesnažil smo preučevali souporabo hidrodinamične kavitacije (HC) ter napredne oksidacije z H_2O_2 in UV svetlobo. Vzorci pitne vode so vsebovali huminsko kislino, barvilo metilen-modro ter mikroonesnažila (metaldehid, diatrizojsko kislino in ioheksol). Najprej smo vzorce oksidirali z H_2O_2 (doze med 1 in 12 mg L^{-1}) ter UV svetlobo (doze med 300 in 2800 mJ cm^{-2}), kasneje pa pod istimi pogoji še ob souporabi HC, sprožene s šobo ter zaslonkami z različnim številom odprtin (4, 8 in 18). Ob souporabi HC se je odstranjevanje huminske kisline izboljšalo za 5–15%, razbarvanje barvila metilen-modro za 5–20 % in metaldehida za približno 10%. Predvsem v primerih, ko je bila začetna UV absorbanca vode relativno visoka (več kot 0,050 cm^{-1} pri valovni dolžini 254 nm) ter pri visokem razmerju med koncentracijami onesnažil in dozami uporabljenih oksidantov, je souporaba HC izboljšala hidrodinamične pogoje v fotolitskem reaktorju, povečala izpostavljenost H_2O_2 UV svetlobi ter povečala učinkovitost odstranjevanja izbranih onesnažil, kar kaže obetavna izhodišča za nadaljnje raziskave na tem področju.